

An Embryonic Staging Table for *In Ovo* Development of *Eublepharis macularius*, the Leopard Gecko

PATRICK A.D. WISE,^{1*} MATTHEW K. VICKARYOUS,²
AND ANTHONY P. RUSSELL¹

¹Department of Biological Sciences, University of Calgary, Calgary, Alberta, Canada

²Department of Biomedical Sciences, Ontario Veterinary College, University of Guelph, Guelph, Ontario, Canada

ABSTRACT

Squamates constitute a major vertebrate radiation, representing almost one-third of all known amniotes. Although speciose and morphologically diverse, they remain poorly represented in developmental studies. Here, we present an embryonic staging table of *in ovo* development for the basal gekkotan *Eublepharis macularius* (the leopard gecko) and advocate this species as a laboratory-appropriate developmental model. *E. macularius*, is a hardy and tractable species of relatively large body size (with concomitantly relatively large eggs and embryos), that is widely available and easy to maintain and propagate. Additionally, *E. macularius* displays a body plan appropriate to the study of the plesiomorphic quadrupedal condition of early pentadactylous terrestrial amniotes. Although not unexpected, it is worth noting that the morphological events characterizing limb development in *E. macularius* are comparable with those described for the avian *Gallus gallus*. Therefore, *E. macularius* holds great promise as a model for developmental studies focusing on pentadactyly and the formation of digits. Furthermore, it is also attractive as a developmental model because it demonstrates temperature-dependent sex determination. The staging table presented herein is based on an all-female series and represents the entire 52 day *in ovo* period. Overall, embryogenesis of *E. macularius* is similar to that of other squamates in terms of developmental stage attained at the time of oviposition, patterns of limb and pharyngeal arch development, and features of the appearance of scalation and pigmentation, indicative of a conserved developmental program. Anat Rec, 292:1198–1212, 2009. © 2009 Wiley-Liss, Inc.

Key words: *Eublepharis macularius*; staging table; development; squamata; gekkota; eublepharidae

Data from staging tables are frequently used in studies of the origin and evolution of major morphological transitions in phylogenetic lineages. One distinct limitation of this approach is that many putatively model taxa

have highly specialized body forms. For example, some of the most commonly used reptiles for developmental studies are the domestic chicken (*Gallus gallus*), Japanese quail (*Coturnix c. japonicus*), American alligator

Additional Supporting Information may be found in the online version of this article.

Grant sponsor: Alberta Ingenuity Postdoctoral Fellowship; Contract grant number: 200500526; Grant sponsor: NSERC Discovery; Contract grant number: 9745.

*Correspondence to: Patrick A.D. Wise, Department of Biological Sciences, University of Calgary, 2500 University Dr. N.W.

Calgary, AB T2N 1N4, Canada. Fax: 403-289-9311. E-mail: padwise@ucalgary.ca

Received 2 October 2008; Accepted 7 May 2009

DOI 10.1002/ar.20945

Published online in Wiley InterScience (www.interscience.wiley.com).

TABLE 1. Summary of embryonic staging data available for squamates

Species	Embryonic series covered	Source
Iguania		
Agamidae		
<i>Agama impalearis</i>	Pre- and post-oviposition	Mouden et al. (2000)
<i>Calotes versicolor</i>	Post-oviposition	Muthukkaruppan et al. (1970)
	Pre-oviposition	Thapliyal et al. (1973)
<i>Chamaeleo lateralis</i>	Pre- and post-oviposition	Blanc (1974)
<i>Chamaeleo bitaeniatus</i>	Post-oviposition	Pasteels (1956)
	Post-oviposition	Milaire (1957)
Iguanidae		
<i>Anolis sagrei</i>	Pre- and post-oviposition	Sanger et al. (2008b)
<i>Liolaemus t. tenuis</i>	Pre-oviposition	Lemus and Duvauchelle (1966)
	Post-oviposition	Lemus et al. (1981)
<i>Liolaemus gravenhorstii</i>	Pre- and post-oviposition	Lemus (1967)
Scleroglossa		
Lacertidae		
<i>Lacerta viridis</i>	Post-oviposition	Dhouailly and Saxod (1974)
<i>Podarcis (Lacerta) agilis</i>	Pre- and post-oviposition	Peter (1904)
	Post-oviposition	Rieppel (1994)
<i>Podarcis (Lacerta) muralis</i>	Post-oviposition	Dhouailly and Saxod (1974)
<i>Podarcis (Lacerta) vivipara</i>	Intra-uterine	Dufaure and Hubert (1961)
Scincidae		
<i>Mabuya megalura</i>	Intra-uterine	Pasteels (1956)
Anguidae		
<i>Anguis fragilis</i>	Cleavage	Nicolas (1904)
	Gastrulation and neurulation	Ballowitz (1905)
	Neurulation to closure of the amnion	Meyer (1910)
Serpentes		
<i>Python sebae</i>	Post-oviposition	Boughner et al. (2007)
<i>Natrix natrix</i>	Uncertain	Krull (1906)
	Uncertain	Vielhaus (1907)
<i>Natrix tessellata</i>	Uncertain	Korneva (1969)
<i>Thamnophis s. sirtalis</i>	Intra-uterine	Zehr (1962)
<i>Naja kaouthia</i>	Post-oviposition	Jackson (2002)
<i>Vipera aspis</i>	Intra-uterine	Hubert and Dufaure (1968)
Scincidae		
<i>Hemiergis spp.</i>	Intra-uterine (incomplete coverage)	Shapiro (2002)
Gekkonidae		
<i>Hemidactylus turcicus</i>	Post-oviposition (incomplete coverage)	Werner (1971)
<i>Paroedura picta</i>	Post-oviposition	Noro et al. (2009)
<i>Ptyodactylus hasselquistii guttatus</i>	Post-oviposition (incomplete coverage)	Werner (1971)
<i>Sphaerodactylus argus</i>	Post-oviposition (incomplete coverage)	Werner (1971)

(*Alligator mississippiensis*), common snapping turtle (*Chelydra serpentina*), and red-eared slider turtle (*Trachemys scripta*). None of these taxa is representative of the plesiomorphic quadrupedal condition of terrestrial amniotes. This is particularly problematic for studies seeking to address issues such as the evolution of digits and development of the autopodium (e.g., Bininda-Emonds et al., 2007). Nevertheless, many (although not all) reptiles have a major advantage over therian mammals in which they retain the primitive *in ovo* mode of development, allowing easy access to embryos without surgically compromising breeding females. Accordingly, an oviparous reptilian model taxon with a relatively generalized body plan and limb structure that is easily maintained, bred, and raised, will provide a valuable addition to evolutionary and developmental studies exploring the assembly of the amniote ground plan.

Non-ophidian squamates (hereafter referred to as lizards) are one of the most diverse (approaching 4,500 species; Zug et al., 2001; Pianka and Vitt, 2003) and morphologically variable lineages of reptiles. Although not entirely without representation—partial to complete embryonic staging tables are available for several taxa,

including *Lacerta vivipara* (Dufaure and Hubert, 1961), *Calotes versicolor* (Muthukkarruppan et al., 1970; Thapliyal et al., 1973), and *Liolaemus gravenhorstii* (Lemus et al., 1981) (refer Table 1 for a synoptic overview)—no single taxon of lizard has been widely adopted as a laboratory-amenable developmental model. Most previous studies have focused on locally available species (e.g., European investigators have emphasized indigenous lacertids; Dufaure and Hubert, 1961; Dhouailly and Saxod, 1974), or have targeted taxa with highly specialized morphologies (e.g., to investigate limb reduction; Raynaud, 1985; Shapiro, 2002; Shapiro et al., 2003) or aspects of reproductive biology (e.g., viviparity; Shine, 1983; Shine and Thompson, 2006) to address specific questions. Recently, two captive raised lizard taxa have been documented in the literature and proposed as useful developmental models. First, Sanger et al. (2008a,b) proposed the genus *Anolis* as a model for exploring the development of evolutionary and morphological diversification within a lineage. The *Anolis* model is specifically aimed at investigating the subtleties of ecomorphological variation within a single adaptive radiation. Additionally, *Anolis* is the subject of a genome sequencing project



Fig. 1. *E. macularius*, the leopard gecko, (Eublepharidae, Gekkota). Left lateral view of an adult female. Scale bar = 5 mm.

(Losos et al., 2005). Second, Noro et al. (2009) described embryonic development in the gekkonid gekkotan *Paroedura pictus*, and demonstrated the utility of this taxon for egg windowing and *in ovo* access to the embryo (Noro et al., 2009). Unlike more deeply nested gekkotans (including *P. pictus*), eublepharids retain eyelids (other geckos develop a spectacle). Furthermore, *Eublepharis macularius* exhibits temperature-dependent sex determination for which the temperature ranges determining gender are well documented (Bull, 1987; Viets et al., 1993, 1994).

Here, we provide a detailed description of *in ovo* development for a second gekkotan species, the leopard gecko, *E. macularius* (Eublepharidae) (Fig. 1). Gekkotans reside phylogenetically near the base of the squamate radiation (Fig. 2), and thus, can be considered good candidates for establishing fundamental developmental data for this clade. Among gekkotans, eublepharids are relatively basal (Gamble et al., 2008), and are characterized as oviparous, terrestrial taxa with a conservative morphology (i.e., no limb reduction or trunk elongation), and pentadactylous limbs primitively lacking subdigital adhesive pads.

E. macularius is a medium sized lizard (average snout vent length for specimens encountered in the wild is 120 mm; Minton, 1966) indigenous to parts of eastern Afghanistan, Pakistan, and western India (Grismer, 1988, 1991; Szczerbak and Golubev, 1996). The native habitat is flat rocky desert and sparse grassland between 600 and 2,500 m in elevation in localities dominated by clay-rich soils (Smith, 1935; Szczerbak and Golubev, 1996). Stomach contents of wild-caught *E. macularius* reveal unidentified crickets, grasshoppers, beetles, scorpions, and lizards (Smith, 1935; Minton, 1966; Schifter, 1967), and available evidence suggests that it is a wide ranging forager (Van Damme and Vanhooydonck, 2001; Bauer, 2007).

E. macularius is well known to reptile hobbyists (herpetoculturalists) as a tractable and hardy species and has a proven history in captivity (Wagner, 1974; Thorogood and Whimster, 1979; Wise, 1997; de Vosjoli et al., 2005; Seuffer et al., 2005; refer below). Hatchlings are easily raised to adulthood, enabling multigenerational

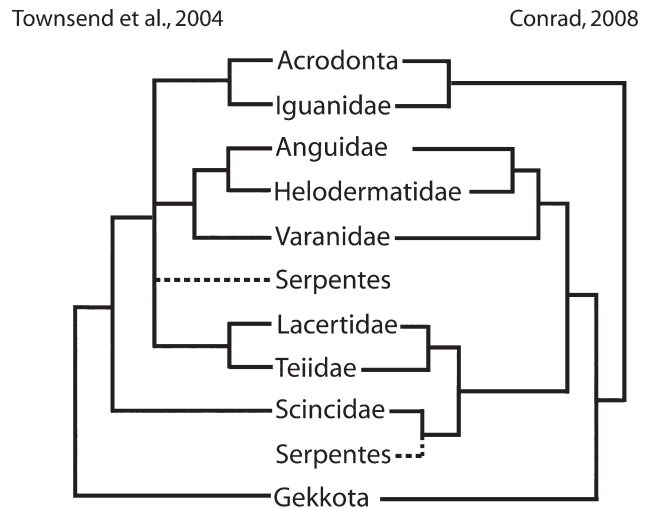


Fig. 2. Phylogenetic position of the Gekkota (Gekkonidae in the works being cited) as resolved in two recent hypothesis of the relationships of the higher taxa of squamates. The pattern revealed by Townsend et al. (2004), based upon molecular data, places the Gekkota in a basal position in the phylogeny; that of Conrad (2008), based upon morphological data, places the Gekkota as basal among the scleroglossans, with the Iguania being the sister taxon to the Scleroglossa.

breeding lines to be established. The commercial abundance of this species in Europe and North America obviates the need to procure wild-caught individuals (except for the occasional revitalization of breeding stock) and minimizes parasite and other health-related issues that are often attendant with wild caught individuals (Sanger et al., 2008a). In addition, *E. macularius* is amenable to selective breeding programs, with a number of phenotypic variants already established, including 16 color variants, and one size strain.

Although clutch size is small (normally two, less commonly one; Werner, 1972; Kratochivl and Frynta, 2006; Kratochivl and Kubicka, 2007), females are able to produce multiple clutches throughout the breeding season,

making eggs from an individual animal available over a period of 2–4 months. The eggs, and consequently the embryos, are relatively large (eggs: 25 × 12 mm) and this is an attractive feature for those who wish to perform microsurgical manipulations on *in ovo* embryos.

Previously *E. macularius* has been used in studies of gene expression and function (Valleley et al., 2001; Gamble et al., 2006), endocrinology (Janes et al., 2007), reproductive physiology (Bull, 1987; Viets et al., 1993, 1994; Rhen et al., 2000), central nervous system development (Coomber et al., 1997), inter and intrasexual differences (Crews et al., 1998), tissue grafts and tail regeneration (Whimster, 1978), and middle ear structure and function (Werner and Wever, 1972). Thus, establishment of this taxon as a developmental model capitalizes on *E. macularius*, already well established use as a relatively well-characterized experimental model organism.

Details of the embryonic development of *E. macularius*, however, have not heretofore been investigated. Our description of *in ovo* development for an all female series provides the necessary information to facilitate future *evo-devo* studies.

MATERIALS AND METHODS

Information on captive maintenance and reproductive husbandry, serving as a guide for those who wish to establish a breeding colony, is available as Supporting Information.

Embryos were sacrificed in accordance with Canadian Council on Animal Care guidelines (University of Calgary animal care protocol BI2006-37), and fixed in 10% neutral buffered formalin for 48 hr at room temperature (RT). After rinsing in running tap water for 24 hr, embryos were stored in 70% ethanol (at RT). Morphological staging follows the criteria set out by Dufaure and Hubert (1961) and Muthukkarruppan et al. (1970) for lizards, with additional features adopted from the avian staging table of Hamburger and Hamilton (1951). Embryos were photographed with a Canon Digital Rebel camera equipped with Canon 5:1 macro and Tamron 1:1 macro lenses, and with a Nikon D200 camera mounted on a Nikon SZ800 dissecting microscope. Images were cropped and resized using Adobe Photoshop version 5.0.

RESULTS

In Ovo Embryonic Development

The following data are derived from observations on 92 embryos. A total of 111 eggs were incubated at 28°C ± 1°C (the all-female-producing temperature; Bull, 1987; Viets et al., 1993, 1994). Ten eggs were infertile, and nine other embryos succumbed to unknown causes *in ovo*, yielding a fertility rate of 91% and a survival rate of 83%. Developmental time from oviposition to hatching at this temperature is 52 ± 2 days. A minimum of two embryos were examined for each developmental day.

Staging Criteria

To the greatest extent possible, the stages and staging criteria established for *E. macularius* are aligned with those previously established for other lizards (Dufaure and Hubert, 1961; Muthukkarruppan et al., 1970); and correlated with the morphological criteria presented in

more recent studies (Sanger et al., 2008a; Noro et al., 2009) (Table 2). In addition, we provide a framework for comparison with a well-characterized developmental model, the avian *G. gallus*, by correlating key features of limb morphogenesis between *E. macularius* and *G. gallus*.

For captive bred and raised *E. macularius*, oviposition occurs at stages 28–29 and hatching at stage 42. As for other reptiles (including birds), chronological length of each stage is variable (Table 3) and hence the use of absolute time is unsuitable for making intra- and interspecific comparisons (Billet et al., 1985). Details of limb development are important for establishing staging criteria throughout most of the *in ovo* developmental period (stages 28–41). Other valuable morphological criteria for staging include the development of the pharyngeal arches (including maxillary and mandibular branches of the first arch; stages 28–34), the eye and adnexa (stages 28–37), and scale formation and skin pigmentation (stages 36–42). The final stage of *in ovo* development (stage 42) is characterized by the external appearance of the paired egg teeth.

Before egg deposition (stage 28 or 29), development has already progressed through the blastula and gastrula stages and is well into organogenesis, with almost complete formation of the neural tube and initiation of formation of the secondary brain vesicles. Pharyngeal arch formation has begun and somitogenesis is also well underway, with ~ 33 pairs evident at the time of laying. Distinct condensations representing the presumptive optic and auditory (otic) vesicles are also evident, and the gut is closed.

Descriptions of each embryonic stage are presented as brief sentences that list key features in a cranial to caudal sequence. Only those features that have changed from the previous stage are mentioned.

Stage 28 (Fig. 3a–c)

Cranial. The mesencephalon forms a conspicuous bulge (Fig. 3a) at the back of head (in the region of the future parietal). The neural tube is open cranially as far anteriorly as the cranial edge of the metencephalon (Fig. 3c).

Eye. The eye is round, the margins of the choroid fissure contact one another, and have begun to fuse (Fig. 3b).

Facial. Facial primordia are present but are not yet fused together.

Flexures and rotation. Cranial flexure is well underway, with the axes of the forebrain and hindbrain forming an acute angle (Fig. 3a). The cervical flexure is a broad curve, compounded by the rotation of the body, with the point of rotation being located just anterior to, or at the level of, the forelimb buds. During body rotation, the head turns to the left so that ultimately the embryo comes to lie on its right side.

Pharyngeal arches. Pharyngeal clefts 1 and 2 are open, whereas pharyngeal cleft 3 is present as a groove that is beginning to widen (Fig. 3b).

Limbs. Forelimb buds are present as small protuberances, whereas the hindlimb buds are not yet visible.

Body. The heart is visible as a single, curved endocardial tube protruding from the thoracic cavity (Fig. 3b).

TABLE 2. A Comparison of Equivalent Developmental Stages in Various Lizard Taxa and the Avian *Gallus gallus*

	<i>Lacerta vivipara</i> (Dufaure and Hubert, 1961)	<i>Calotes versicolor</i> (Muthukkarruppan et al., 1970)	<i>Chamaleo lateralis</i> (Blanc, 1974)	<i>Podarcis muralis</i> (Dhouailly and Saxod, 1974)	<i>Podarcis viridis</i> (Dhouailly and Saxod, 1974)	<i>Anolis sagrei</i> (Sanger et al., 2008b)	<i>Paroedura pictus</i> (Noro et al., 2009)	<i>Gallus gallus</i> (Hamburger and Hamilton, 1951)	Correlation of limb development events between <i>E. macularius</i> and <i>G. gallus</i>
ST 28	ST 26 ST 27 ST 28	ST 27 ST 28	ST 27	ST 26 D 1	ST 26		D 0 D 1 D 2	HH 17	<i>G. gallus</i> : hind-limb bud develops; in both <i>E. macularius</i> and <i>G. gallus</i> : fore-limb buds with comparable morphologies
ST 29	ST 29	ST 29				SS 4-5	D 3	HH 18-20	<i>E. macularius</i> : hindlimb bud develops; <i>G. gallus</i> : hind-limb bud becomes larger than forelimb bud
ST 30	ST 30	ST 30	ST 31 ST 33	D 3 D 7	D 4	SS 5 SS 6	D 4-11	HH 21-23	
ST 31	ST 31	ST 31					D 12-17	HH 24	<i>E. macularius</i> : fore- and hind-limb buds similar in size; in both taxa: autopodium develops discrete paddle shape in both <i>E. macularius</i> and <i>G. gallus</i> : zeugopodium and stylopodium become distinct in both <i>E. macularius</i> and <i>G. gallus</i> : digits develop (may begin slightly earlier in <i>G. gallus</i>)
ST 32	ST 32	ST 32		D 9	D 10	SS 6-7	D 18-19	HH 25	
ST 33	ST 33	ST 33				SS 7-8	D 20-23	HH 26	
				D 12	D 18				

TABLE 2. A Comparison of Equivalent Developmental Stages in Various Lizard Taxa and the Avian *Gallus gallus* (continued)

	<i>Lacerta vivipara</i> (Dufaure and Hubert, 1961)	<i>Calotes versicolor</i> (Muthukkarruppan et al., 1970)	<i>Chamaleo lateralis</i> (Blanc, 1974)	<i>Podarcis muralis</i> (Dhouailly and Saxod, 1974)	<i>Podarcis viridis</i> (Dhouailly and Saxod, 1974)	<i>Anolis sagrei</i> (Sanger et al., 2008b)	<i>Paroedura pictus</i> (Noro et al., 2009)	<i>Gallus gallus</i> (Hamburger and Hamilton, 1951)	Correlation of limb development events between <i>E. macularius</i> and <i>G. gallus</i>
ST 34	ST 34	ST 34	ST 36	D 15-16		SS 8-9	D 24-25	HH 29-33	
ST 35	ST 35	ST 35	ST 38	D 19		SS 8-10	D 26	HH 34	
ST 36	ST 36	ST 36				SS 10-11	D 27	HH 35	in both <i>E. macularius</i> and <i>G. gallus</i> .
ST 37	ST 36	ST 37			D 28	SS 12	D 28-29	HH 36	in both <i>E. macularius</i> and <i>G. gallus</i> : phalanges develop
ST 38	ST 37	ST 38		D 21		SS 13-14	D 30+?	HH 37+	in both <i>E. macularius</i> and <i>G. gallus</i> : claws develop
ST 39	ST 38	ST 39	ST 42	D 25-30		SS 15-16			in both <i>E. macularius</i> and <i>G. gallus</i> : scale formation and pigmentation
ST 40	ST 39	ST 40		D 42		SS 17	D 35		
ST 41	ST 40	ST 41				SS 18	D 40-49		
ST 42	ST 40	ST 42	ST 44	D 46	D 60	SS 19	D 50-80	HH 46	

Stages and staging criteria for lizards are drawn from the work of Dufaure and Hubert (1961: *Podarcis vivipara*) and Muthukkarruppan et al. (1970: *Calotes versicolor*) and are based primarily on the state of limb and pharyngeal arch development. In the later stages of development (40-42), pigmentation and scalation were also emphasized. In some instances it was necessary to interpret developmental information that were not presented in the standardized staging mode. Stages not represented by the embryonic series are left blank. See text for details.

ST, embryonic stage based on Dufaure and Hubert (1961: *Podarcis vivipara*) and Muthukkarruppan et al. (1970: *Calotes versicolor*); see text for details. D, days post-oviposition.

SS, embryonic stage based on Sanger et al. (2008b),

HH, embryonic stage based on Hamburger and Hamilton (1951).

TABLE 3. Duration of embryonic stages and snout vent length (SVL) measurements for the 92 specimens of *Eublepharis macularius* used in this study

Stage	Days of <i>in ovo</i> development	Duration of stage (days \pm 8 hr)	Number of embryos examined	Minimum SVL (mm)	Maximum SVL (mm)
28	0–1	1	4	3	4.4
29	4–6	2	3	4.2	8.7
30	1–8	7	11	12.3	15.2
31	9–16	7	6	12.2	15.1
32	12–14	2	3	14.4	16.8
33	14–17	3	2	17.6	17.6
34	12–22	10	16	16.4	25.9
35	21–26	5	6	27.6	30.8
36	25–28	3	2	29.9	29.9
37	25–33	8	2	33.8	33.8
38	23–31	8	6	35.1	40.9
39	33–35	2	4	38.2	42.4
40	36–42	6	9	37.5	44.7
41	36–45	9	9	43.5	49.6
42	44–54	8	9	47.7	58.1

Note that stages are not congruent with absolute time (*in ovo* development), and hence a range of stages may coexist on the same day of development.

Stage 29 (Fig. 3d–f)

Eye. The choroid fissure is closed.

Facial. The nasolabial groove becomes conspicuous as the facial primordia grow closer together.

Flexures and rotation. The rotation point of the body is located at the level of the forelimb buds.

Pharyngeal arches. Pharyngeal clefts 1, 2, and 3 are open, whereas pharyngeal cleft 4 appears as a groove late in stage 29 (Fig. 3f).

Limbs. Forelimb and hindlimb buds are evident as distinct protuberances (Fig. 3d,e). Forelimb buds are larger than hindlimb buds.

Stage 30 (Fig. 3g–j)

Cranial. The paired mesencephalic bulges are each equal in length and diameter to the eye when viewed laterally. There are also paired visible prominences in the nasal region and swellings in the frontal area that are narrow and moderately convex. Anterior closure of the neural tube has progressed caudally as far as the posterior edge of the mesencephalon (Fig. 3j).

Eye. The first traces of pigment begin to appear (Fig. 3i).

Flexures and rotation. Cervical flexure approaches a 90-degree angle. The location of body rotation varies from the level of the forelimb buds to just posterior to them.

Pharyngeal arches. Pharyngeal cleft 1 begins to close ventrally, but remains open dorsally. Pharyngeal clefts 2, 3, and 4 remain open; a groove marks the position of pharyngeal cleft 5 (Fig. 3i). Pharyngeal arch 2 overlaps

pharyngeal cleft 2, obscuring it in lateral view (Fig. 3i). The maxillary process of the first pharyngeal arch has grown rostrally to lie adjacent to the rostral margin of the eye when the head is viewed laterally (Fig. 3i).

Limbs. The limb buds are plate-like with a distinct border at the edges (Fig. 3h). The forelimb is slightly longer than the hindlimb, and is curved and directed caudally. The hindlimb is still straight, directed ventrally, and its long axis is held perpendicular to the body axis (Fig. 3j).

Stage 31 (Fig. 3k–m)

Cranial. Nasal processes are present as a pair of swellings (Fig. 3m). The frontal prominence is visible as a single median structure but is weakly developed.

Eye. The eye is kidney-shaped and fully pigmented, and the choroid fissure is no longer visible (Fig. 3m).

Flexures and rotation. Cervical flexure makes a 90-degree angle, and the point of body rotation progresses from lying just posterior to the front limbs to immediately anterior to the hindlimbs.

Pharyngeal arches. Pharyngeal arches 1 and 2 are well-defined, whereas pharyngeal arch 3 is less prominent. Pharyngeal clefts 1 and 2 are present, whereas pharyngeal clefts 3–5 have disappeared. The maxillary process of pharyngeal arch 1, visible at the rostroventral margin of the eye (Fig. 3m), contacts the lateral nasal process and develops into a mound-like mass in the area of the future maxilla. The contralateral mandibular processes of pharyngeal arch 1 meet in the midline and begin to fuse. In lateral profile, the rostrum has the

Fig. 3. Embryonic development of *E. macularius*, stages 28–31. Each row of panels begins with a view of the whole embryo, followed by multiple panels providing a higher magnification view of important morphological features characteristic of the stage. Scale bar for the intact embryos = 2 mm. Scale bars for the subsequent panels = 1 mm. Unless otherwise stated, all images represent left lateral views. Stage 28 (a–c) with a closer view of the heart and pharynx (b), and the neural tube in dorsal view (c). Stage 29 (d–f) with a closer view of

the forelimb bud (e), and pharynx (f). Stage 30 (g–j) illustrating a closer view of the forelimb bud (h), pharynx (i), and the fusing neural tube in dorsal view (j). Stage 31 (k–m) with a closer view of the forelimb (l), and craniofacial region (m). aer, apical ectodermal ridge; cf, choroid fissure; e, eye; et, endocardial tube; np, nasal prominence; nt, neural tube; op, otic placode; pa, pharyngeal arch; pc, pharyngeal cleft; pg, pharyngeal groove.

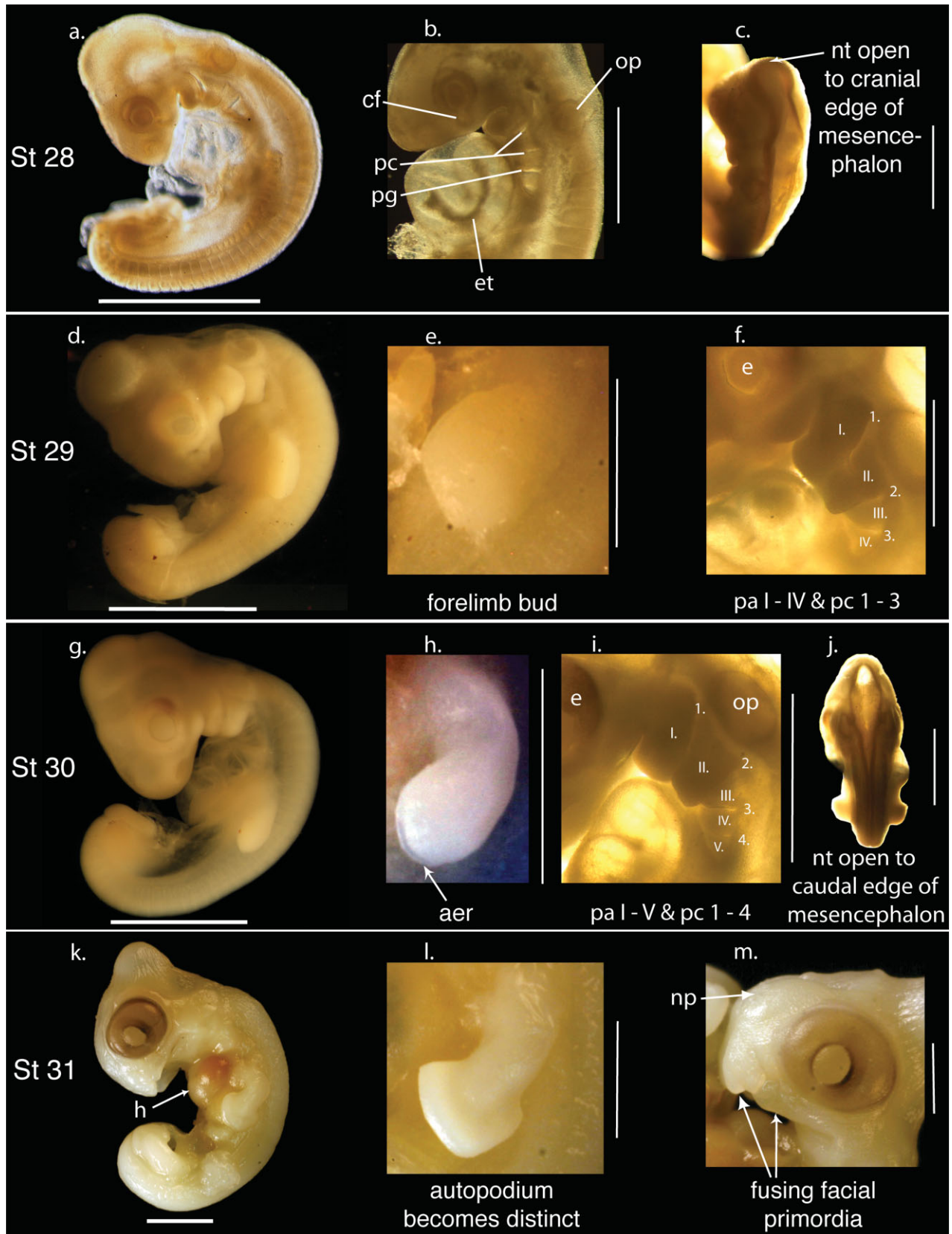


Fig. 3.

appearance of a hooked beak with the fusing mandibular processes being 25% the length of the craniofacial ("upper jaw") region.

Limbs. Forelimbs and hindlimbs are similar in appearance, and the autopodium is flat, paddle-like, and roughly triangular in shape (Fig. 3l). Neither the stylopodium nor the zeugopodium are clearly differentiated.

Stage 32 (Fig. 4a–c)

Cranial. The frontal swelling is a single median eminence.

Eye. The pupil has moved closer to the rostral margin than the caudal margin.

Facial. The nasolabial grooves have disappeared (Fig. 4c).

Pharyngeal arches. Pharyngeal arches 2 and 3 remain visible, but pharyngeal arches 4 and 5 have become flush with the body wall (Fig. 4c). The contralateral mandibular processes are completely fused to form the developing lower jaw, which is now 50% the length of the craniofacial region (Fig. 4c).

Limbs. The forelimbs and hindlimbs are now divided into three distinctive segments: stylopodium, zeugopodium, and autopodium (Fig. 4b). The autopodium lacks digital condensations.

Body. The heart begins to withdraw into the thoracic cavity but remains externally visible as a slight bulge.

Somites. The somites are no longer visible.

Stage 33 (Fig. 4d,e)

Cranial. The external auditory meatus first appears as a slight indentation on the lateral surface, caudal and slightly ventral to the position of the eye.

Eye. The pupil approaches a central position within the eye.

Pharyngeal arches. The lower jaw is now about 75% the length of the craniofacial region.

Limbs. Condensations of digits 2, 3, and 4 are visible in the autopodium of both the forelimbs and hindlimbs (Fig. 4e). The autopodium is of uniform dorsal to palmar/plantar thickness.

Stage 34 (Fig. 4f–h)

Cranial. Swelling develops in the area of the presumptive parietal bone (Fig. 4f,h). The indentation of the external auditory meatus continues to deepen, but visible evidence of a tympanum is lacking.

Eye. The developing upper and lower eyelids project from the perimeter of the eye as a thin and ribbon-like sheet of tissue (Fig. 4f). Between the developing eyelids, the exposed portion of the eye is oval in shape.

Pharyngeal arches. By the end of stage 34, the lower jaw is equal in length to the craniofacial region.

Limbs. Condensations demarcating all five digits are visible in each if the forelimb and hindlimb buds (Fig. 4g). Interdigital webbing is complete at the beginning of the stage, but has slightly concave margins by the end of stage 34. The digits are visibly thicker than the interdigital areas of the autopodium.

Body. The heart no longer protrudes from the thoracic cavity.

Stage 35 (Fig. 4i–k)

Cranial. The pineal eye is visible on the dorsal surface of the head between the eyes. Paired, obliquely-oriented swellings in the area of the presumptive frontal bones develop, forming an open "V" in dorsal view (Fig. 4k). Swellings in the area of the presumptive parietal bone are prominent and kidney-shaped in dorsal view. The tympanum is evident by the end of this stage.

Eye. The developing upper and lower eyelids partially cover the eye to the level of the pupil (Fig. 4i).

Facial. The external nares are visible as faint depressions.

Limbs. The interdigital webbing is deeply incised, and digits 1 and 5 are noticeably shorter than digits 2, 3, and 4 (Fig. 4j).

Scales. The caudal half of the embryo shows the initial appearance of scales. These are most noticeable on the tail.

Stage 36 (Fig. 5a–c)

Cranial. The swellings in the area of the presumptive nasal bone diminish in size. The contralateral swellings in the area of the presumptive frontal bone fuse, and the swelling in the area of the presumptive parietal begins to diminish in size. The fronto-parietal fontanelle is clearly visible. The head is almost as deep as it is long.

Facial region. The preorbital region of the head is shorter than, or equal to, the maximum diameter of the eye (Fig. 5c).

Pharyngeal arches. The lower jaw is longer than the craniofacial region (mandibular prognathism; Fig. 5a,c).

Limbs. Webbing is now absent between the digits, and phalangeal segments begin to appear in the digits (Fig. 5b).

Stage 37 (Fig. 5d–f)

Eye. The middle portion of the ocular (distal) margin of both upper and lower eyelids begins to thicken (Fig. 5d,f). By the end of the stage, the thickened region of the ocular margin of both upper and lower eyelids has spread to the caudal margin of the eye.

Facial. The length of the preorbital region of the head now exceeds the maximum diameter of the eye (Fig. 5f).

Pharyngeal arches. The upper and lower jaws are the same length (Fig. 5f).

Limbs. Claws are present on all digits by the end of this stage (Fig. 5e).

Scales. Scales are present on the hindlimb, with the exception of the toes.

Stage 38 (Fig. 5g–i)

Cranial. Swellings in the area of the presumptive frontal bone are weakly developed. The swelling in the area of the presumptive parietal bone is initially distinct and contributes to the dome-like profile of the head when viewed laterally (Fig. 5g,i), but by the end of the stage it begins to merge with the contour of the head and becomes less distinct. The length of the head is almost equal to the length of the trunk.

Eye. The thickening of the ocular margin of both the upper and lower eyelids spreads to the rostral margin of the eye.

Facial. The preorbital length of the head is about 150% the length of the maximum diameter of the eye (Fig. 5i).

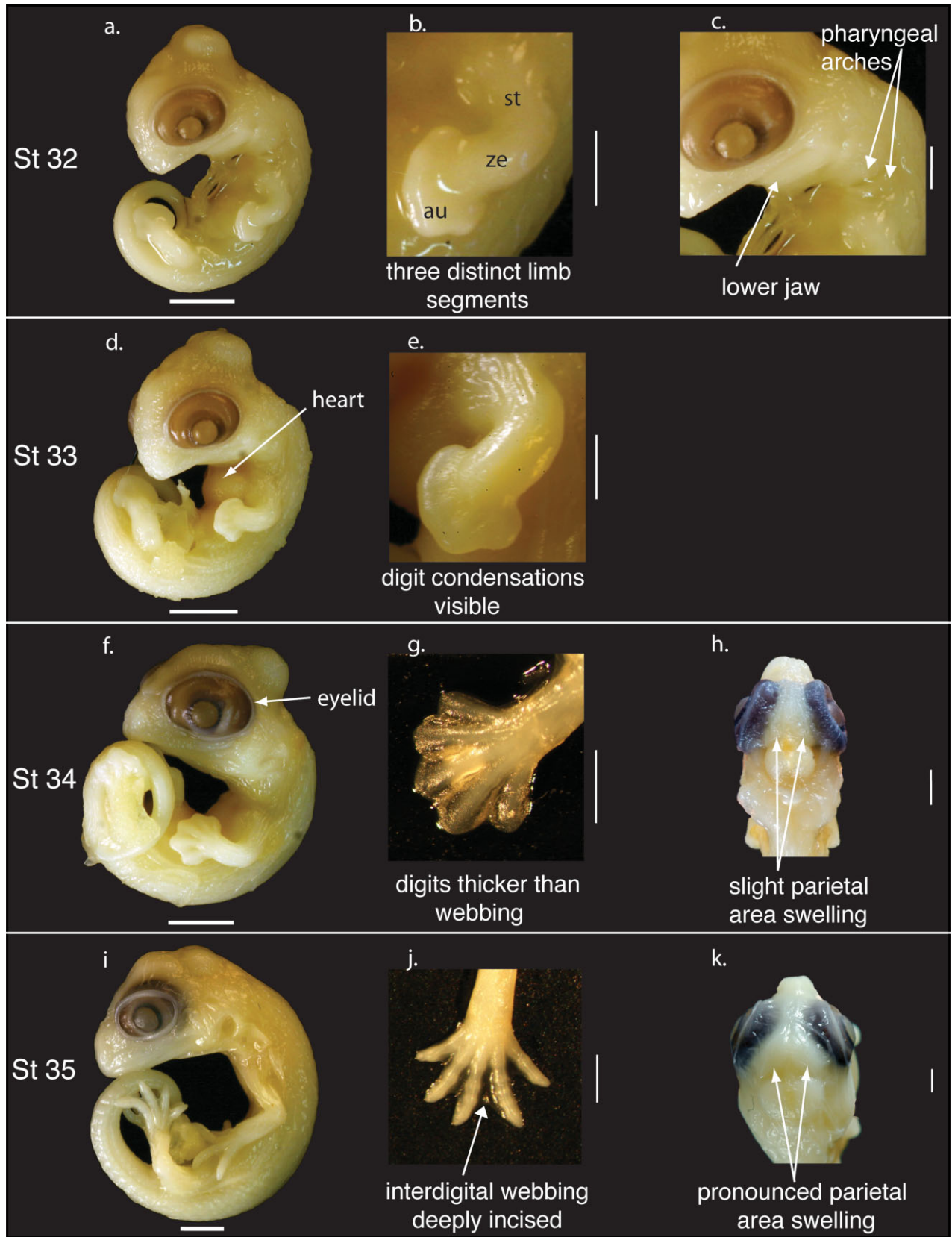


Fig. 4. Embryonic development of *E. macularius*, stages 32–35, arrayed as for Fig. 3. Scale bar for the intact embryos = 2 mm. Scale bars for the inset panels = 1 mm. Unless otherwise stated, all images represent left lateral views. Stage 32 (a–c) showing a closer view of the forelimb (b) and pharynx (c). Stage 33 (d,e) depicting a closer view

of the forelimb bud (e). Stage 34 (f–h) illustrating a closer view of the manus (g) and the head in dorsal view (h). Stage 35 (i–k) showing a closer view of the manus (j), and the head in dorsal view (k). au, autopodium; st, stylopodium; ze, zeugopodium.

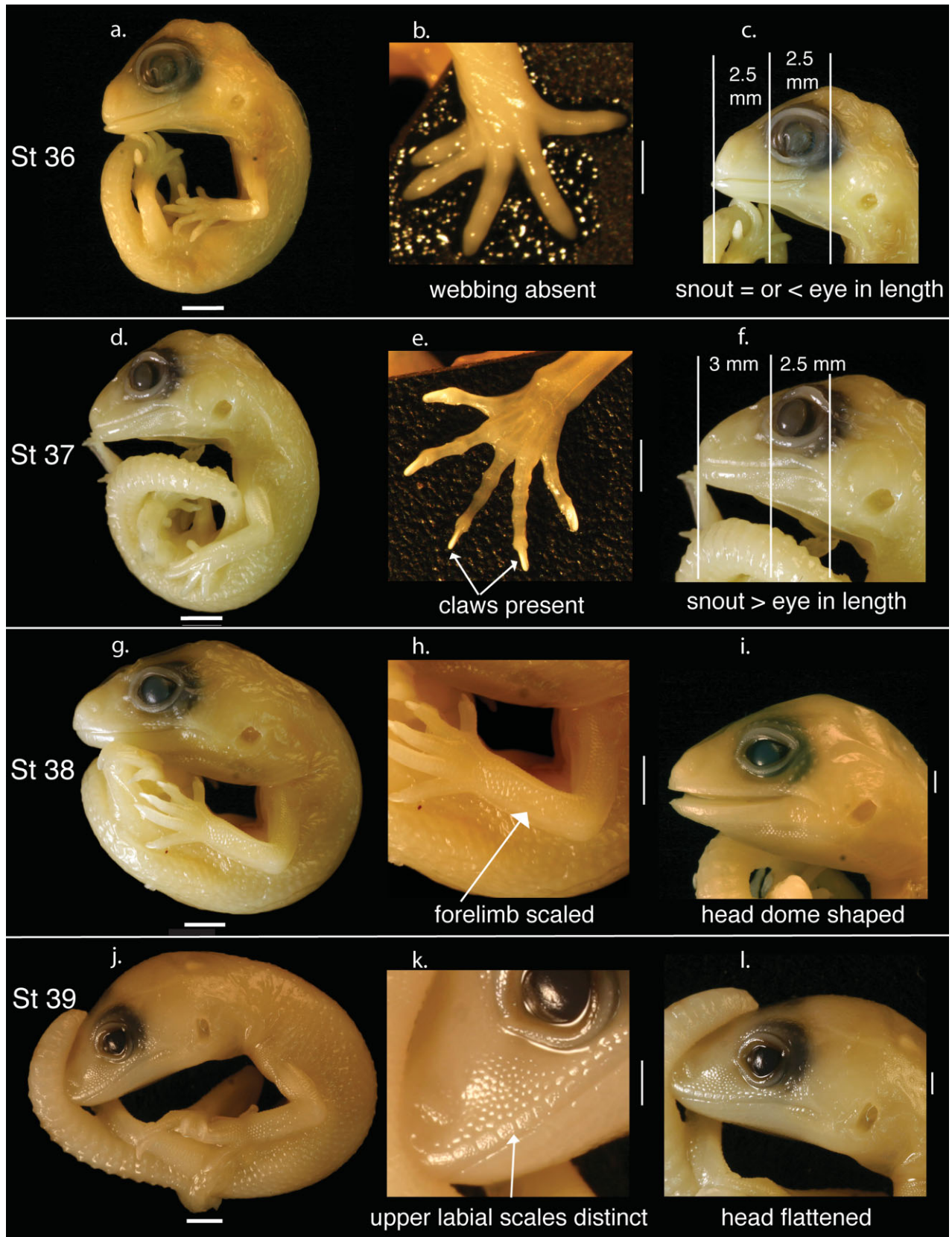


Fig. 5. Embryonic development of *E. macularius*, stages 36–39, arrayed as for Fig. 3. Scale bar for the intact embryos = 2 mm. Scale bars for the inset panels = 1 mm. Unless otherwise stated, all images represent left lateral views. Stage 36 (a–c) depicting a closer view of

the manus (b) and head (c). Stage 37 (d–f) showing a closer view of the manus (e) and head (f). Stage 38 (g–i) illustrating a closer view of forelimb scalation (h) and the head (i). Stage 39 (j–l) depicting a closer view of the pattern of craniofacial scalation (k), and the head (l).

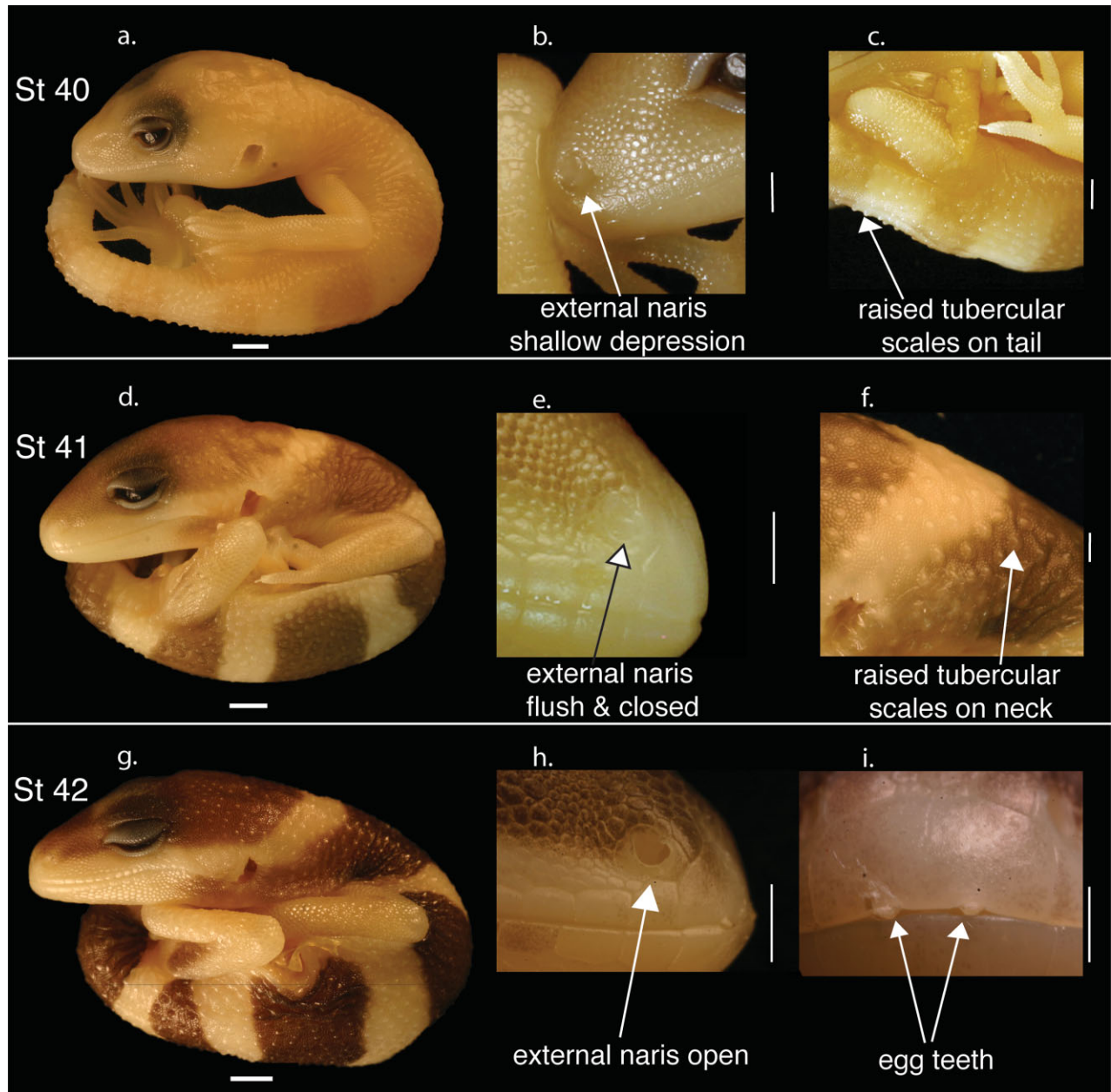


Fig. 6. Embryonic development of *E. macularius*, stages 40–42, arrayed as for Fig. 3. Scale bar for the intact embryos = 2 mm. Scale bars for the inset panels = 1 mm. Unless otherwise stated, all images represent left lateral views. Stage 40 (a–c) showing a closer view of the craniofacial scalation (b) and scales on the tail (c). Stage 41 (d–f)

illustrating a closer view of the external nares in right lateral view (e) and the tubercular scales of the head (f). Stage 42 (g–i) depicting a closer view of the external nares in right lateral view (h) and the egg teeth in cranial view (i).

Scales. The forelimbs begin to express scales during this stage and are completely scaled by its end (Fig. 5h). The ventral side of the head also develops scales, with the labial scales on the lower jaw becoming faintly visible.

Stage 39 (Fig. 5j–l)

Cranial. The swellings in the area of the presumptive parietal and frontal bones are fused. The head has a flatter appearance in lateral view (Fig. 5j,l).

Scales. Scale development is evident over the entire head, with labial scales becoming faintly visible on the upper jaw (Fig. 5k).

Stage 40 (Fig. 6a–c)

Scales. The body and limbs are fully scaled, with tubercular scales forming conical elevations on the caudal half of the body (Fig. 6c). On the cranial half of the body, these scales remain flat (Fig. 6a,b).

Pigmentation. The juvenile, banded pigmentation pattern begins to develop on the body, and is weakly visible on the forelimb (Fig. 6a).

Overall, the embryo has attained 30%–50% of its hatching length.

Stage 41 (Fig. 6d–f)

Cranial. The head begins to flatten across the postorbital region, and becomes more like that of a hatchling in its proportions.

Facial. The external naris is present as a distinct pit, but remains sealed by tissue that is flush with the surface of the snout (Fig. 6e).

Pharyngeal arches. Notches in the rostralmost region of the upper jaw for the egg teeth may or may not be present, but the egg teeth are not yet visible.

Scales. Tubercular scales with well developed keels cover the body, and keel development progresses in a caudal to rostral direction along the neck (Fig. 6f). Scales on the head remain flat.

Pigmentation. At the start of stage 41, the juvenile banded pigmentation pattern is distinct across the body, whereas that of the forelimb is present as spots on the stylopodium only. By the end of stage 41, the complete juvenile pigmentation pattern is expressed (Fig. 6d).

Overall, the embryo grows from 50% to 100% of its hatching length through this stage.

Stage 42 (Fig. 6g–i)

Cranial. In lateral profile, the head is depressed, and is similar in form to that of a hatchling (Fig. 6g).

Facial. The external nares open during this stage (Fig. 6h).

Pharyngeal arches. Paired egg teeth become visible between the upper and lower jaw and grow to protrude beyond the jaw line (Fig. 6i).

Scales. All of the tubercular scales of the head express keels by the end of this stage (hatching).

DISCUSSION

This description of *in ovo* development for an all-female series of *E. macularius* is the first for a eublepharid gekkotan and the first embryonic staging series that is controlled for sex. It is significant to note that even under controlled conditions, embryos of the same absolute (chronological) age are not always at the same stage of external morphological development (Table 3). To maximize the interspecific utility of the *E. macularius* embryonic data, we have aligned our stages with, and used the staging criteria of, earlier studies (Dufaure and Hubert, 1961; Muthukkarruppan et al., 1970). We have also correlated our stages with several recently described lizard embryonic series (Sanger et al., 2008b; Noro et al., 2009), and with limb development of *G. galus* (Table 2).

The sequence of morphological events for captive bred *E. macularius* is broadly congruent with previously established sequences of embryonic development in other lizards, although several minor differences are noteworthy. Oviposition occurs at stages 28–29, corresponding to the “Early limb-bud” stage of Sanger et al. (2008b; their stages 4–5) for *Anolis* spp. In the gekkotan *P. pictus*, ovi-

position occurs at stages 22–24 (Noro et al., 2009), whereas lacertids and *C. versicolor* the eggs are laid at stage 26 or 27.

Compared with other lizards, the pattern of scalation develops relatively earlier in *E. macularius*, with the forelimbs completely scaled by stage 38. In contrast, forelimb scalation is not complete until stage 39 in *L. vivipara* (Dufaure and Hubert, 1961) and stage 40 in *C. versicolor* (Muthukkarruppan et al., 1970). Similarly, head scales appear earlier in *E. macularius* (at stage 39) than *C. versicolor* (stage 40; Muthukkarruppan et al., 1970). However, opening of the external nares is delayed in *E. macularius* (stage 42) compared with *C. versicolor* (stage 41; Muthukkarruppan et al., 1970).

As noted for other oviparous lizards (e.g., Noro et al., 2009), *E. macularius* provides an accessible model for the study of pentadactylus limb development. The basic sequence of *E. macularius* limb morphogenesis is consistent with the events reported for *A. sagrei* (Sanger et al., 2008b) and *P. pictus* (Noro et al., 2009), and closely parallels limb morphogenesis in the avian *G. galus* (Hamburger and Hamilton, 1951; refer Table 2). The following description broadly applies to all three lizard taxa, although methodological differences in establishing staging criteria preclude a more detailed analysis at this time. By stage 29, both forelimb and hindlimb buds (Fig. 3d,e) have developed, with the forelimb buds appearing first. Following a period of elongation (up to stage 30; Fig. 3h), the limb begins to regionalize. In general, the autopodium is distinct by stage 31 (Fig. 3l), and by stage 32, the stylopodium and zeugopodium are discretely identifiable (Fig. 4b). During stage 33 (Fig. 4e), digit condensations first become visible in the autopodial paddle. At stage 34 (Fig. 4g), the interdigital webbing starts to regress and the digits become better defined. Further regression of the webbing occurs in stages 35–37 (Figs. 4j, 5b,e), along with the initial expression of claws.

Similar to crocodylians, many turtles, and various other lizards, *E. macularius* exhibits temperature-dependent sex determination (Viets et al., 1993, 1994; Valleley et al., 2001). Hence, we are able to control for sex. In this instance, we have focused on embryos raised at the all-female-producing temperature of 28°C (Bull, 1987; Viets et al., 1993, 1994). Future investigations will document embryonic development at the male-biased incubation temperatures, although there is no constant temperature that yields 100% males (Viets et al., 1993). As *E. macularius* does not exhibit any sexually dimorphic morphological characteristics until several months after hatching (Wise et al., unpublished), it is hypothesized that the features used as staging criteria will not differ between males and females. However, gene expression studies investigating the role of *Sox9* in *E. macularius* have been used to determine sex before hatching (Valleley et al., 2001). At the earliest stage sampled, stage 34, *Sox9* is expressed in the urogenital organs of embryos incubated at both the all-female and male-biased temperatures. By stage 37, presumptive female gonads no longer express *Sox9*, whereas presumptive male gonads do. This work opens the door for future contributions aimed at furthering our understanding of the evolution and development of amniote sex determination.

This description of *E. macularius* prehatching development expands and enhances the number of published

reptilian staging series. Both *E. macularius* and *P. pictus* are members of the Gekkota, a diverse circumglobal lineage of more than 1,000 species (Kluge, 1967). Significantly, whereas *P. pictus* is a deeply nested form that has apparently reverted to a secondarily terrestrial lifestyle, *E. macularius* is primitively terrestrial, more basal, and lacks the digital modifications and proportionality evident in pad-bearing geckos (both those that express adhesive pads and those that have secondarily lost them; Russell et al., 1997). Consequently, comparative developmental studies of these two gekkotans provide for opportunities to investigate the evolutionary developmental biology of one of the largest and most basal squamate radiations (Townsend et al., 2004; Conrad, 2008).

ACKNOWLEDGMENTS

The authors thank the anonymous reviewers whose constructive criticisms greatly improved the quality of this manuscript.

LITERATURE CITED

- Ballowitz E. 1905. Die gastrulation bei der blindschleiche (*Anguis fragilis* L.). Z Wiss Zool 83:1–26.
- Bauer AM. 2007. Foraging biology of the Gekkota: life in the middle. In: Reilly SM, McBrayer LB, Miles DB, editors. Lizard ecology. Cambridge: Cambridge University Press. p 371–404.
- Billet F, Gans C, Maderson PFA. 1985. Why study reptilian development? In: Gans C, Billet F, Maderson PFA, editors. Biology of the reptilia. Development A. Vol. 14. New York: Wiley. p 1–40.
- Bininda-Emonds ORP, Jefferey JE, Sánchez-Villagra MR, Hanken J, Colbert M, Pieau C, Selwood L, ten Cate C, Raynaud A, Osabutey CK, Richardson MK. 2007. Forelimb-hindlimb developmental timing changes across tetrapod phylogeny. BMC Evol Biol 7: 182–188.
- Blanc F. 1974. Table de développement de *Chamaeleo lateralis* gray, 1831. Ann Embryol Morphol 7:99–115.
- Boughner JC, Buchtova M, Fu K, Diewert V, Hallgrimsson B, Richman JM. 2007. Embryonic development of *Python sebae*—I: staging criteria and macroscopic skeletal morphogenesis of the head and limbs. Zool 110:212–230.
- Bull JJ. 1987. Temperature-sensitive periods of sex determination in a lizard: similarities with turtles and crocodylians. J Exp Zool 241:143–148.
- Conrad JL. 2008. Phylogeny and systematics of Squamata (Reptilia) based on morphology. Bull Am Mus Nat Hist 310:1–182.
- Coomer P, Crews D, Gonzalez-Lima F. 1997. Independent effects of incubation temperature and gonadal sex on the volume and metabolic capacity of brain nuclei in the leopard gecko (*Eublepharis macularius*), a lizard with temperature-dependent sex determination. J Comp Neurol 380:409–421.
- Crews D, Sakata J, Rhen T. 1998. Developmental effects on intersexual and intrasexual variation in growth and reproduction in a lizard with temperature-dependent sex determination. Comp Biochem Physiol C 119:229–241.
- de Vosjoli P, Tremper R, Klingenberg R. 2005. The herpetoculture of leopard geckos: twenty seven generations of living art. California: Advanced Visions Inc.
- Dhouailly D, Saxod R. 1974. Les stades du développement de *Lacerta muralis* Laurent entre la ponte et l'éclosion. Bull Soc Zool France 99:489–494.
- Dufaure JP, Hubert J. 1961. Table de développement du lézard vivipare: *Lacerta (Zootoca) vivipara* jacquin. Arch Anat Microsc Morphol Exp 50:309–328.
- Gamble T, Aherns JL, Card V. 2006. Tyrosinase activity in the skin of three strains of albino gecko (*Eublepharis macularius*). Gekko 5:39–44.
- Gamble T, Bauer AM, Greenbaum E, Jackman TR. 2008. Out of the blue: a novel, trans-Atlantic clade of geckos (Gekkota, Squamata). Zool Scr 37:355–366.
- Grismer LL. 1988. Phylogeny, taxonomy, classification, and biogeography of eublepharid geckos. In: Estes R, Pregill G, editors. Phylogenetic relationships of the lizard families. Stanford: Stanford University Press. p 369–469.
- Grismer LL. 1991. Cladistic relationships of the lizard *Eublepharis turcmenicus* (Squamata: Eublepharidae). J Herpetol 25: 251–253.
- Hamburger V, Hamilton HL. 1951. A series of normal stages in the development of the chick embryo. J Morphol 88:49–92.
- Hubert J, Dufaure JP. 1968. Table de développement de la vipère aspic, *Vipera aspis*. Bull Soc Zool France 93:135–148.
- Jackson K. 2002. Post-ovipositional development of the monocled cobra, *Naja kaouthia* (Serpentes: Elapidae). Zool 105:203–214.
- Janes DE, Bermudez D, Guillette LJ, Wayne ML. 2007. Estrogens induced male production at a female-producing temperature in a reptile (leopard gecko, *Eublepharis macularius*) with temperature-dependent sex determination. J Herpetol 41:9–15.
- Kluge AG. 1967. Higher taxonomic categories of gekkonid lizards and their evolution. Bull Am Mus Nat Hist 135:1–64.
- Korneva LG. 1969. Embryonic development of the water snake (*Natrix tessellata*). Zool Zhour 98:110–120.
- Kratochvíl L, Kubička L. 2007. Why reduce clutch size to one or two eggs? Reproductive allometries reveal different evolutionary causes of invariant clutch size in lizards. Funct Ecol 21: 171–177.
- Kratochvíl L, Frynta D. 2006. Body-size effect on egg size in eublepharid geckos (Squamata: Eublepharidae), lizards with invariant clutch size: negative allometry for egg size in ectotherms is not universal. Biol J Linn Soc Lond 88:527–532.
- Krull J. 1906. Die Entwicklung der Ringelnatter (*Tropidonotus natrix* Boie) vom ersten Aufstehen des Proamnion bis zum Schlusse des Amnion. Z Wiss Zool 85:107–155.
- Lemus AD. 1967. Contribucion al estudio de la embriologia de reptiles chilenos. II. Tabla de desarrollo de la lagartija vivipara *Liolaemus gravenhorsti*. Biol 40:39–61.
- Lemus AD, Duvauchole CR. 1966. Desarrollo intrauterino de *Liolaemus tenuis tenuis* (Dumeril y Bibron). Contribucion al estudio del desarrollo embriologico de reptiles chilenos. Biol 39:80–98.
- Lemus D, Illanes J, Fuenzalida M, De La Vega YP, Garcia M. 1981. Comparative analysis of the development of the lizard *Liolaemus tenuis tenuis*. II. A series of normal postlaying stages in embryonic development. J Morphol 169:337–349.
- Losos J, Braun E, Brown D, Clifton S, Edwards S, Gibson-Brown J, Glenn T, Guillette L, Main D, Minx P, Modi W, Pfrender M, Pollock D, Ray D, Shedlock A, Warren W. 2005. Proposal to sequence the first reptilian genome: the green anole lizard, *Anolis carolinensis*. Available at: <http://www/genome.gov/Pages/Research/Sequencing/SeqProposals/GreenAnoleLizardAmericanAlligatorSeq.pdf>.
- Meyer E. 1910. Über die Entwicklung der Blindschleiche (*Anguis fragilis* L.) vom Auftreten des Proamnion bis zum Schlusse. Z Wiss Zool 94:447–487.
- Milaire J. 1957. Contribution a la connaissance morphologique et cytologique des bourgeons de membres chez quelques reptiles. Arch Biol (Liege) 68:429–512.
- Minton SA. 1966. A contribution to the herpetology of West Pakistan. Bull Am Mus Nat Hist 134:27–184.
- Mouden EE, Bons J, Pieau C, Renous S, Znari M, Boumezzough A. 2000. Table de développement embryonnaire d'un lézard agamidé, *Agama impalearis* Boettger, 1874. Ann Sci Nat Zool 21:93–115.
- Muthukkarruppan VR, Kanakambika P, Manickavel V, Veeraraghavan K. 1970. Analysis of the development of the lizard, *Calotes versicolor*, I. a series of normal stages in the embryonic development. J Morphol 130:479–490.
- Nicolas A. 1904. Reserches sur l'embryologie des reptiles. IV. La segmentation chez l'ovet. Arch Biol Paris 20:611–658.
- Noro M, Uejima A, Abe G, Manabe M, Tamura K. 2009. Normal developmental stages of the Madagascar ground gecko *Paroedura pictus* with special reference to limb morphogenesis. Dev Dyn 238:100–109.

- Pasteels J. 1956. Une table analytique du développement des reptiles. I. Stades de gastrulation chez cheloniens et lacertiliens. *Ann Soc Roy Zool Belg* 87:217–241.
- Peter K. 1904. Normentafeln zur entwicklungsgeschichte der zauneidechse (*Lacerta agilis*). Vol. 4. In: Fischer G. editor. Jena: Keibel's Normentafeln. p 1–65.
- Pianka ER, Vitt LJ. 2003. Taxonomic summary of lizard genera. In: Pianka ER, Vitt LJ, editors. *Lizards: windows to the evolution of diversity*. Berkeley: University of California Press. p 299–302.
- Raynaud A. 1985. Development of limbs and embryonic limb reduction. In: Gans C, Billett F, editors. *Biology of the reptilia. Development B*. Vol. 15. New York: Wiley. p 59–148.
- Rhen T, Sakata JT, Zeller M, Crews D. 2000. Sex steroid levels across the reproductive cycle of female leopard geckos, *Eublepharis macularius*, from different incubation temperatures. *Gen Comp Endocrinol* 118:322–331.
- Rieppel O. 1994. Studies on skeleton formation in reptiles. Patterns of ossification in the skeleton of *Lacerta agilis exigua* Eichwald (reptilia, squamata). *J Herpetol* 28:145–153.
- Russell AP, Bauer AM, Laroia R. 1997. Morphological correlates of the secondarily symmetrical pes of gekkotan lizards. *J Zool* 241:767–790.
- Sanger TJ, Hime PM, Johnson MA, Diani J, Losos JB. 2008a. Laboratory protocols for husbandry and embryo collection of *Anolis* lizards. *Herpetol Rev* 39:58–63.
- Sanger TJ, Losos JB, Gibson-Brown JJ. 2008b. A developmental staging series for the lizard genus *Anolis*: a new system for the integration of evolution, development, and ecology. *J Morphol* 269:129–137.
- Schifter H. 1967. Beobachtungen au panthergecko, *Eublepharis macularius* (Blyth 1854). Vol. 20. Stuttgart: Die Aquarien und Terrarien-Zeitschrift. p 151–154.
- Seufer H, Kaverkin Y, Kirschner A. 2005. *Eublepharis macularius* (Blyth, 1954) leopard gecko. In: Seufer H, Kaverkin Y, Kirschner A, editors. *The eyelash geckos: care, breeding and natural history*. Germany: Kirschner & Seufer. p 110–126.
- Shapiro MD. 2002. Developmental morphology of limb reduction in *Hemiergus* (Squamata: Scincidae): chondrogenesis, osteogenesis, and heterochrony. *J Morphol* 254:211–231.
- Shapiro MD, Hankin J, Rosenthal N. 2003. Developmental basis of evolutionary digit loss in the Australian lizard *Hemiergus*. *J Exp Zool* 297:48–56.
- Shine R. 1983. Reptilian reproductive modes: the oviparity-viviparity continuum. *Herpetologica* 39:1–8.
- Shine R, Thompson MB. 2006. Did embryonic responses to incubation conditions drive the evolution of reproductive modes in squamate reptiles? *Herpetol Monogr* 20:159–171.
- Smith MA. 1935. The fauna of British India including Ceylon and Burma, reptilia and amphibia. Vol. 2. London: Taylor & Francis.
- Szczerbak NN, Golubev ML. 1996. Gecko fauna of the USSR and contiguous regions. In: Golubev ML, Malinsky SA, Translators; Leviton AE, Zug G, editors. *Contributions to herpetology*. Vol. 13. New York: SSAR.
- Thapliyal JP, Singh KS, Chandola A. 1973. Pre-laying stages in the development of Indian garden lizards *Calotes versicolor*. *Ann Embryol Morphol* 6:253–259.
- Thorogood J, Whimster IW. 1979. The maintenance and breeding of the leopard gecko as a laboratory animal. In: Olney PJS, editor. *International zoo yearbook*. Vol. 19. Dorchester: Henry Ling Ltd. p 74–79.
- Townsend TM, Larson L, Louis E, Macey JR. 2004. Molecular phylogenetics of squamata: the position of snakes, amphisbaenians, and dibamids, and the root of the squamate tree. *Syst Biol* 53:735–757.
- Valley EMA, Cartwright EJ, Croft NJ, Markham AF, Coletta PL. 2001. Characterization and expression of *Sox9* in the leopard gecko, *Eublepharis macularius*. *J Exp Zool* 291:85–91.
- Van Damme R, Vanhooydonck B. 2001. Origins of interspecific variation in lizard sprint capacity. *Funct Ecol* 15:186–202.
- Vielhaus T. 1907. Die entwicklung der rhingelnatter (*Tropidonotus natrix* Boie) nach ausbildung der falterform bis zur erhebung des proamnioms. *Z Wiss Zool* 86:55–99.
- Viets BE, Tousignant A, Ewert MA, Nelson CE, Crews D. 1993. Temperature-dependent sex determination in the leopard gecko, *Eublepharis macularius*. *J Exp Zool* 265:579–683.
- Viets BE, Ewert MA, Talent LG, Nelson CE. 1994. Sex determining mechanisms in squamate reptiles. *J Exp Zool* 270:45–56.
- Wagner E. 1974. Breeding the leopard gecko. In: Duplaix-Hall N, editor. *International zoo yearbook*. Vol. 14. Sussex: Ditchling Press Ltd. p 84–86.
- Werner YL. 1972. Observations on eggs of eublepharid lizards, with comments on the evolution of the gekkonoidea. *Zool Meded* 47:211–224.
- Werner YL. 1971. The ontogenetic development of the vertebrae in some gekkonoid lizards. *J Morphol* 133:41–92.
- Werner YL, Wever EG. 1972. The function of the middle ear in lizards: *Gekko gecko* and *Eublepharis macularius* (Gekkonoidea). *J Exp Zool* 179:1–16.
- Whimster IW. 1978. Nerve supply as a stimulator of the growth of tissues including skin. II. Animal evidence. *Clin Exp Dermatol* 3:389–410.
- Wise PAD. 1997. Leopard geckos. *Reptile Life* 1:24–27.
- Zehr DR. 1962. Stages in the normal development of the common garter snake, *Thamnophis sirtalis sirtalis*. *Copeia* 2:322–329.
- Zug GR, Vitt LJ, Caldwell JP. 2001. Tuataras and lizards. In: Zug GR, Vitt LJ, Caldwell JP, editors. *Herpetology: an introductory biology of amphibians and reptiles*. 2nd ed. San Diego: Academic Press. p 465–501.